Carbohydrate Polymers 83 (2011) 676–687

Contents lists available at ScienceDirect

Carbohydrate Polymers

journal homepage: www.elsevier.com/locate/carbpol

Characterization of microcrystalline cellulose prepared from lignocellulosic materials. Part II: Physicochemical properties

Abeer M. Adel[a,*], Zeinab H. Abd El-Wahab[b], Atef A. Ibrahim[a], Mona T. Al-Shemy[a]

[a] Cellulose and Paper Department, National Research Center, Dokki, Cairo, Egypt
[b] Chemistry Department, Faculty of Science(Girl's), Al-Azhar University, P.O. Box 11754, Nasr City, Cairo, Egypt

ARTICLE INFO

Article history:
Received 27 July 2010
Accepted 16 August 2010
Available online 21 August 2010

Keywords:
Microcrystalline cellulose (MCC)
Rice hulls
Bean hulls
Scanning electron microscopy (SEM)
Infrared spectroscopy (FTIR)
Thermogravimetry analysis (TGA) and
X-ray diffraction

ABSTRACT

Microcrystalline cellulose (MCC) is a very important product in pharmaceutics, foods, cosmetics and other industries. In this work, MCC was prepared from rice and bean hulls (RH and BH). Hydrolysis of bleached pulps was carried out using hydrochloric or sulfuric acid to study the effect of the acid used on the properties of the produced MCC. MCC samples prepared from RH and BH were characterized through various techniques, scanning electron microscopy (SEM), infrared spectroscopy (FTIR), thermogravimetry analysis (TGA) and X-ray diffraction and compared with commercial MCC. The mechanical properties of tablets made from MCC of different lignocellulosic materials were tested and compared to a commercial MCC.

© 2010 Elsevier Ltd. All rights reserved.

1. Introduction

Microcrystalline cellulose (MCC) is a purified partially depolymerised non-fibrous form of cellulose that occurs as a white, odourless, tasteless, crystalline powder composed of porous particles. Woody plants and cotton were the major sources of MCC, but cost has made it imperative that other materials be investigated as potential sources. MCC can be made from any material that is high in cellulose ranging from pure cellulose, commercial grade cellulose to lignocellulosic materials. Reports have shown that MCC can be produced from soybean, oath and ricehulls as well as sugar beet pulp (Hanna, Blby, & Miladinove, 2001), bagasse and corn cob (Okhamafe, Ejike, Akinrinola, & Ubane-Ine, 1995), groundnut shell and rice husks (Okhamafe, Igboechi, & Obaseki, 1991), and cereal straw (Jain, Dixit, & Varma, 1993). Indian bamboo (Ofoefule & Chukwu, 1999) and luffa cylindrica (Ohwoavworhua, Kunle, & Ofoefule, 2004) have also been studied as potential sources of MCC (Ejikeme, 2008). Since cellulose from different sources differs in properties (crystallinity, moisture content, surface area and porous structure, molecular weight, etc.) different properties of MCC obtained from different sources are expected; and the conditions of hydrolysis also affect the properties of the obtained MCC (El-Sakhawy & Hassan, 2007). The hydrolysis of cellulose to obtain MCC can be accomplished using mineral acid, enzymes or microorganisms. Although enzymatic methods are desirable because glucose, a useful by-product, is created, these methods are more expensive and create MCC products having a lower crystallinity. Thus acid hydrolysis is the conventional method of choice for manufacturing MCC (Hanna et al., 2001).

Cellulose, obtained as a pulp from fibrous plant materials, consists of amorphous cellulose areas and, additionally, well-ordered crystalline regions. MCC is prepared by treating wood pulp or linters with dilute mineral acid and is described as purified, partially depolymerised cellulose with a degree of polymerisation (DP) below 350. MCC is basically made of crystallites of colloidal size. The crystallites aggregate, forming particles of about $15 \pm 20\,\mu m$ diameter. These aggregates in turn agglomerate during drying of the cellulose slurry, so a final mean particle size between 20 and 200 μm is reached (Picker-Freyer, 2007). MCC, produced from a naturally occurring substance (cellulose) has proven to be stable, safe, and physiologically inert and has revolutionized tableting. Microcrystalline cellulose is one of the few materials used in tableting that combines two properties of tablet vehicle; it can produce very hard tablets and yet these tablets disintegrate rapidly in water due to swelling of the MCC particles and destruction of the bonding forces holding them together (Ejikeme, 2008).

* Corresponding author. Tel.: +20 239805715, fax: +20 23371499.
E-mail address: abeermadel2003@yahoo.com (A.M. Adel).

0144-8617/$ – see front matter © 2010 Elsevier Ltd. All rights reserved.
doi:10.1016/j.carbpol.2010.08.039

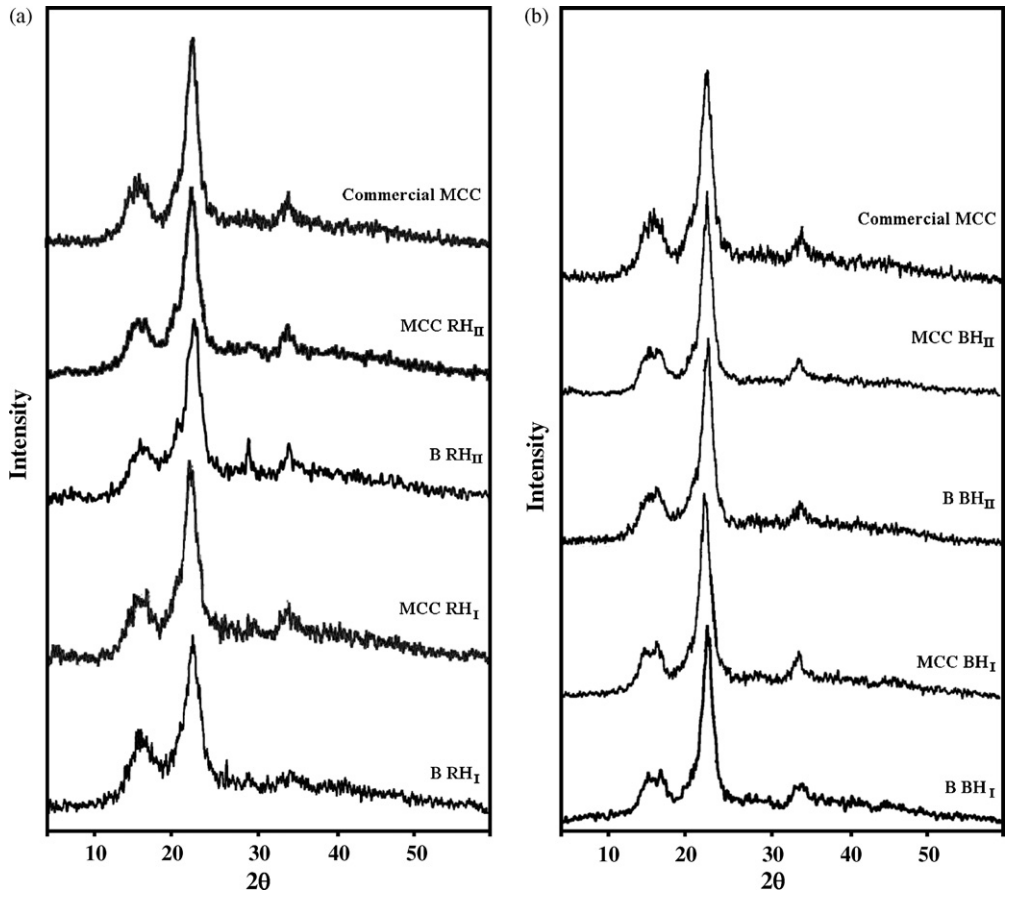

Fig. 1. (a) X-ray diffraction patterns of commercial MCC; (BRH_I) bleached rice hulls pulp pretreated with HCl; (BRH_{II}) bleached rice hulls pulp pretreated with H_2SO_4; (MCC RH_I) microcrystalline cellulose prepared from rice hulls hydrolyzed via HCl and (MCC RH_{II}) microcrystalline cellulose prepared from rice hulls hydrolyzed via H_2SO_4. (b) X-ray diffraction patterns of commercial MCC; (BBH_I) bleached bean hulls pulp pretreated with HCl; (BBH_{II}) bleached bean hulls pulp pretreated with H_2SO_4; (MCC BH_I) Microcrystalline cellulose prepared from bean hulls hydrolyzed via HCl and (MCC BH_{II}) microcrystalline cellulose prepared from bean hulls hydrolyzed via H_2SO_4.

At present, microcrystalline cellulose (MCC) is used in various fields such as pharmacy, cosmetics, food industry, and plastics processing industry. In the powder form, it is used, for example, as a filler and binder in medical tablets and food tablets for dietary purposes. In the gel form, MCC is used as viscosity regulator, a suspending agent, emulsifier in different pastes, creams, etc. (Laka & Chernyavskaya, 2007). The adsorption of the drug on cellulose occurs through hydrogen bonding with the abundant aliphatic hydroxyls and some carboxylic groups, at the particles surface. Since cellulose from different sources differs in properties (crystallinity, moisture content, surface area and porous structure, molecular weight, etc.) different behaviors as drugs carrier are expected for MCC obtained in different ways. On the other hand, physical pre-treatments can also significantly modify MCC powder properties, which result in different dissolution profiles of drugs (Uesu, Pineda, & Hechenleitner, 2000).

The aim of this work was to prepare microcrystalline cellulose (MCC) from rice hulls (RH) and bean hulls (BH). The effect of sulfuric and hydrochloric acid hydrolysis on the prepared MCC was determined. Physical and mechanical properties of MCC prepared from different lignocellulosic materials were carried out. MCC samples were characterized through scanning electron microscope (SEM), infrared spectra (FTIR) and thermal analysis (thermogravimetry, TGA, and derivative thermogravimetry, DTG) and compared with a commercial MCC.

2. Experimental

2.1. Raw material

The raw material used in this work is Rice hull (RH) and bean hull (BH) pretreated with HCl and H_2SO_4 from our previous work (Adel, Abd El-Wahab, Ibrahim, & Al-Shemy, 2010). The pretreatment was carried out at 2% (w/w) mineral acids, at 120 °C for 90 min and 10% consistency. Cellulose microcrystalline LR (Laboratory Rasayan s.d. Fine-Chemicals Ltd., Boisar 401501, India). Sulfuric acid (97%) and hydrochloric acid (37%) were purchased from Abco Chemie Eng. Ltd.

2.2. Characterization of the lignocellulosic material

The chemical compositions and the yield of the pulp, and bleached pulp were determined using the known Tappi standard methods for the different components, namely: T-222 for lignin, T 203 os-61 for α-cellulose, T-211 for ash and T-223 cm-84 for pentosane content. Hollocellulose was quantified using the method of Wise, Murphy, and D'Addieco (1946).

2.3. Pulping and bleaching

The raw material was pulped in a 15 L batch reactor heated by an outer jacket containing electrical wires. The reactor contents

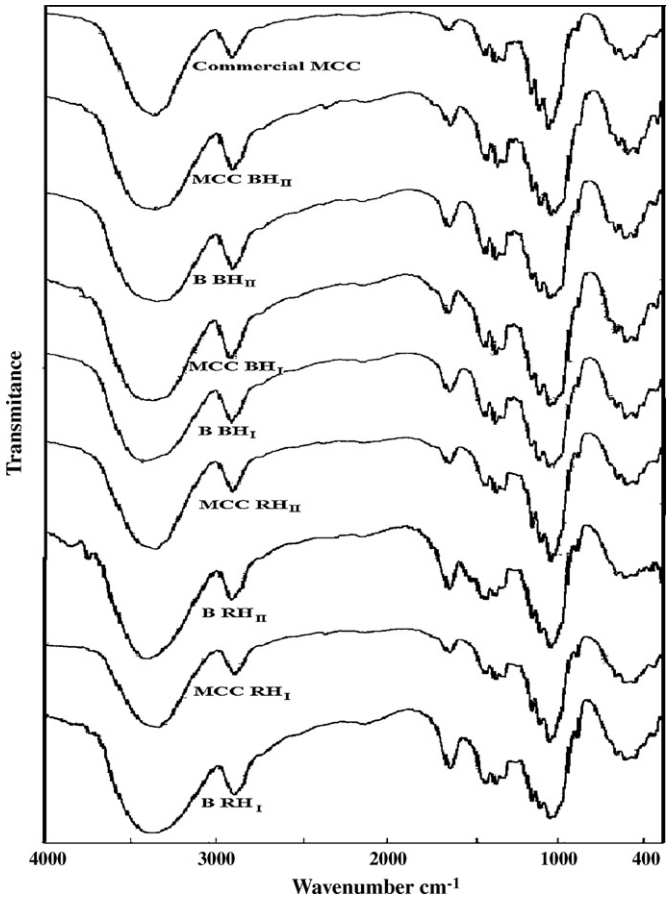

Fig. 2. FTIR spectroscopy for (BRH_I, BBH_I) and (BRH_{II} and BBH_{II}): means bleached rice and bean hulls pretreated with HCl and H_2SO_4, respectively. (MCC RH_I, MCC BH_I) and (MCC RH_{II} and MCC BH_{II}): microcrystalline cellulose prepared from rice and bean hulls hydrolyzed via HCl and H_2SO_4, respectively.

were stirred by rotating the reaction vessel via a motor connected through a rotary axle to a control unit including the required instruments for measurement and control of pressure and temperature. Raw materials were placed in the reactor together with 15 and 10% soda at liquor ratio of 1:6 and 1:5 (raw material:water) for RH and BH samples, respectively, and the autoclave was heated to 170 °C using a heating rate of 1.5 °C/min. and pulped at 170 °C for 180 min (in case of RH) and 120 min (in case of BH). Following pulping process, the pulped material was washed to remove residual pulping liquor and finally, the pulp was allowed to dry to a moisture content of ca. 10% at room temperature. The rice and bean hull pulps were then bleached in polyethylene bags in water bath. Using the conventional three-stage method of hypochlorite bleaching process was carried out. In the hypochlorite stage the pulp was treated with 10% hypochlorite at pH = 11, at 80 °C for 45 min and 10% consistency; followed by the pulp washed with water till neutrality.

The chemical compositions and the yield of the pulp, and bleached pulp were determined and were as follows in Table 1.

2.4. Microcrystalline cellulose preparation

Bleached Rice and bean hulls pulps were hydrolyzed with 2N hydrochloric acid or 2N sulfuric acid under reflux for 45 min (Paralikar & Bhatawdekar, 1988); the liquor ratio was 1:10. The hydrolyzed pulps were thoroughly washed with distilled water and air-dried. Degree of polymerization (DP) of the different samples was determined by viscosity measurement of the samples dissolved in copper–ammonium hydroxide solution (Browning, 1967).

2.5. Analysis

2.5.1. FTIR spectra analysis

Infrared spectra were recorded with a Jasco FT/IR, Nicolet, and Model 670. The samples were measured as thin films using the diffuse reflectance mode of IR spectroscopy. The contribution of CO_2 in air, moisture, and oxygen was eliminated by measuring the background spectra before every sample. Bands were recorded in the region from 4000 to 400 cm^{-1} with Deuterated Triglycine Sulfate (DTGS) detector.

2.6. Thermogravimeteric analysis

TG was recorded by a Perkin-Elmer Thermal Analysis Controller AC7/DX TGA7, using a heating rate of 10 °C/min in nitrogen atmosphere.

2.7. X-ray diffraction

Diffraction patterns were obtained using a Brukur D8 Advance X-ray diffractometer (Germany). The diffraction patterns were recorded using copper (Kα) Target with a secondary monochromator at 40 kV and 40 mA. The crystallinity index (CrI) was calculated via Eq. (1) (Gümüskaya, Usta, & Kirci, 2003):

$$\mathrm{CrI} = \left[\frac{(I_{002} - I_{\mathrm{am}})}{I_{002}}\right] \quad (1)$$

where I_{002} is the intensity of the 0 0 2 peak (at about $2\theta = 26$) and I_{am} is the intensity corresponds to the peak at about $2\theta = 18$.

The average crystallite size of the direction perpendicular to 0 0 2 lattice plane was calculated from the Scherrer equation as follows:

$$L = \frac{k\lambda}{\beta \cos\theta} \quad (2)$$

where L is the size of crystallite (nm), k is the Scherrer constant (0.84), λ is the X-ray wavelength (0.154), β is the FWHM (full width half maximum) of 0 0 2 reflection in radian, and θ is the corresponding Bragg angle (reflection angle) (He, Tang, & Wang, 2007).

2.8. Scanning electron microscopy

Scanning electron microscopy (gold coating, Edwards Sputter Coater, UK) was performed using a Jeol 6310 (Jeol Instruments, Tokyo, Japan) system running at 5–10 keV.

2.9. Preparation of tablets

Tablets were prepared by compacting powders (3 g) in a mold (25 mm diameter); using a uniaxial pressing of 100 MPa and a dwell time of 1 min. Tablets were tested on the same day of preparation, typically 2 h after compaction. This allows compaction and testing to be performed under comparable ambient conditions (temperature and relative humidity).

2.10. Measurement of tablet strength

Diametric tensile testing was performed at 5 mm/min using a LLOYD LR 10 k universal testing machine. Tensile strength was calculated using Eq. (3)

$$\sigma = \frac{2F}{10^6 \pi DT} \quad (3)$$

Table 1
Chemical composition of RH and BH raw materials and their bleached pulps.

	Rice hulls (RH)					Bean hulls (BH)				
	RH	PRH_I	BRH_I	PRH_{II}	BRH_{II}	BH	PBH_I	BBH_I	PBH_{II}	BBH_{II}
Yield %	–	41.29	77.58	26.55	75.72	–	56.95	73.84	50.38	89.01
Hollocellulose %	63.66	84.72	91.67	82.51	87.25	78.37	93.18	94.16	94.00	95.00
α-Cellulose %	30.98	68.24	76.64	67.00	72.32	51.87	84.48	86.16	86.56	87.13
Pentosane %	32.67	16.70	15.02	15.51	14.93	26.49	8.71	8.00	8.00	7.87
Lignin %	16.21	12.00	2.39	10.91	3.81	10.42	6.03	1.29	4.03	1.01
Ash %	16.52	4.04	2.98	5.01	4.48	3.36	2.63	0.74	1.87	0.12
Silica in ash %	13.40	–	–	–	–	–	–	–	–	–
Extracted %	2.12	–	–	–	–	0.29	–	–	–	–

RH means (rice hulls raw materials); $PRH_{I,II}$ means (pulped rice hull pretreated with HCl and H_2SO_4, respectively); BH means (bean hulls raw materials); $PBH_{I,II}$ means (pulped bean hull pretreated with HCl and H_2SO_4, respectively); $BRH_{I,II}$ means (bleached rice hulls pulp pretreated with HCl and H_2SO_4, respectively); $BBH_{I,II}$ means (bleached bean hulls pulp pretreated with HCl and H_2SO_4 respectively).

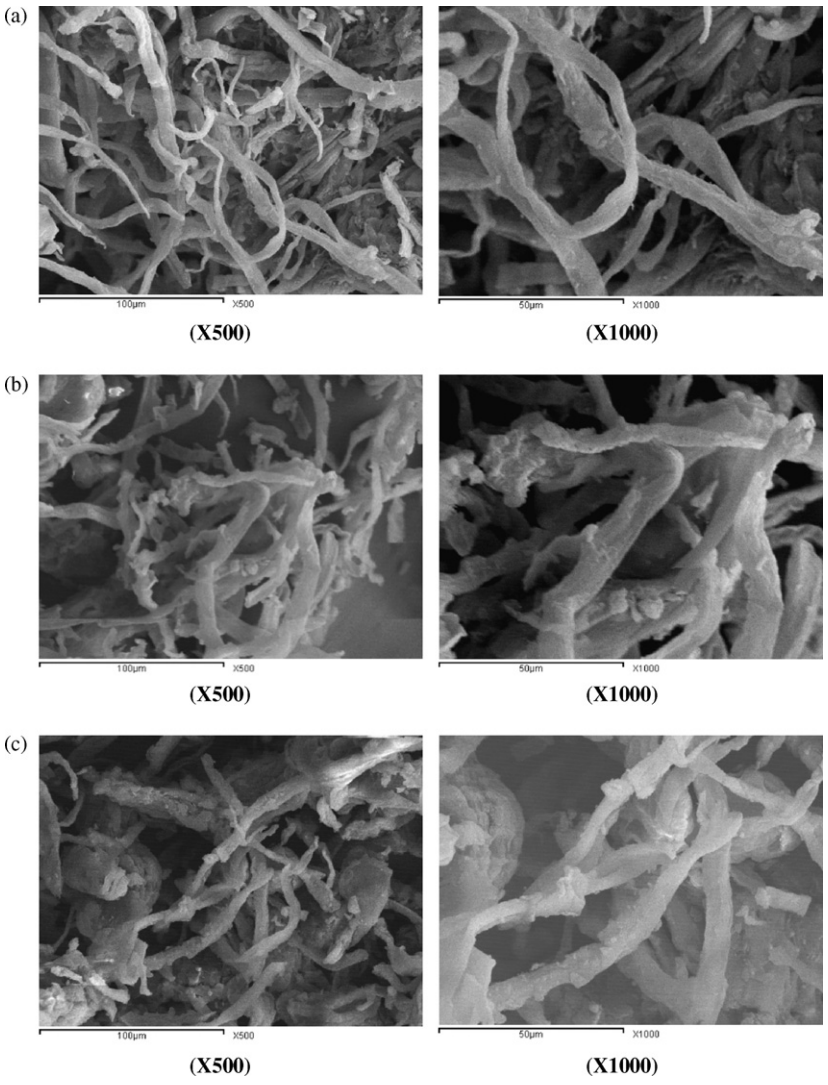

Fig. 3. SEM graphs of (a) BRH_I; (b) MCC RH_I; (c) BRH_{II}; (d) MCC RH_{II}; (e) BBH_I; (f) MCC BH_I; (g) BBH_{II}; (h) MCC BH_{II}; (i) commercial MCC.

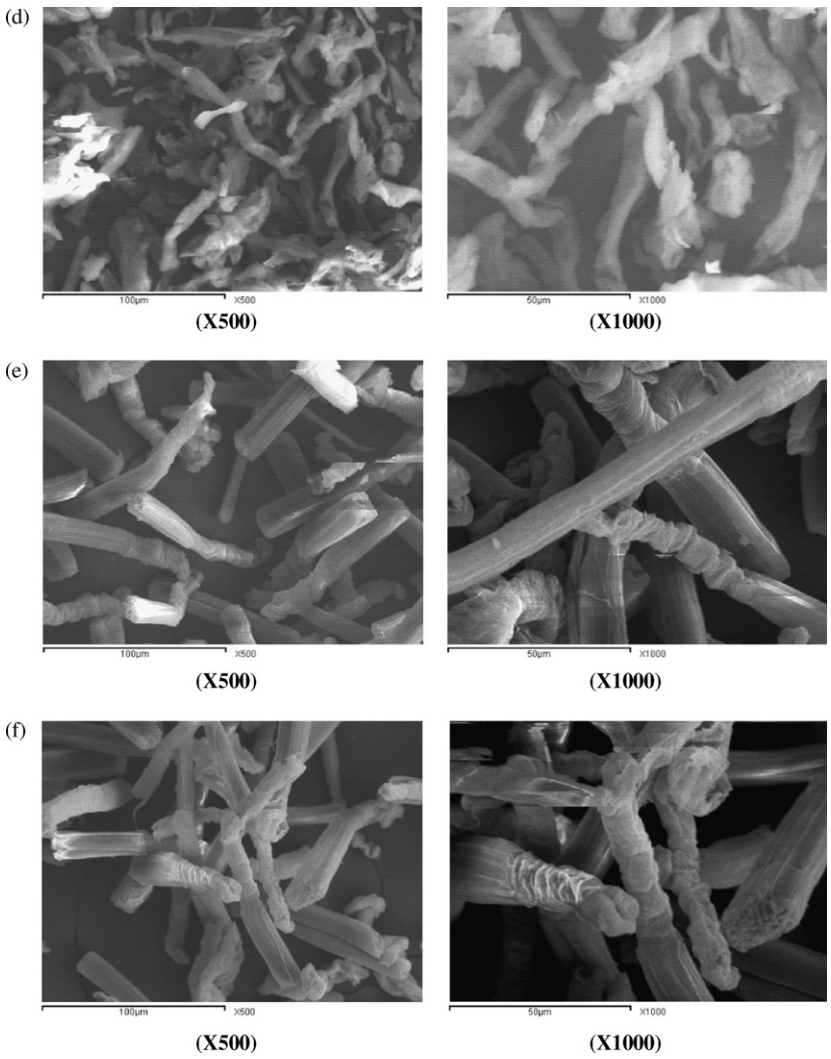

Fig. 3. (*Continued*)

In Eq. (3), σ is the tensile strength (MPa), F is the breaking force (N), D is the tablet diameter (m) and T is the thickness of tablet (m) (Sun, 2008).

2.11. Hardness test of tablets

The hardness of tablets was measured using a WOLPERT Hardness tester HI 2004 according to the DIN 53 456 standard.

2.12. Tablet density

Each tablet was accurately weighed to 0.1 mg and the diameter and the thickness of each tablet were measured to 0.01 mm. Tablet density, ρ_{tablet}, was calculated from tablet diameter, thickness and weight (Sun, 2008).

2.13. Particle size analysis

A sieve-shaker (VEB MLW, Germany) was used for this assessment. Test sieves ranging from 850 to 50 μm were arranged in a descending order. A 20 g quantity of MCC powders was placed on the top sieve and the set-up was shaken for 5 min. The weight of material retained on each sieve was determined. The average diameter was computed by using Eq. (4) (Ohwoavworhua & Adelakun, 2005):

$$\text{Average diameter} = \left[\frac{\sum(\%\,\text{retained}) \times (\text{mean aperture})}{100}\right] \quad (4)$$

3. Results and discussion

3.1. Hydrolysis of bleached rice and bean hull pulps

Hydrolysis of the different kinds of pulps to prepare MCC was carried out using sulfuric or hydrochloric acids. Preliminary experiments showed that these pulps reach constant weight loss and level-off degree of polymerization (LODP) after their reflux with acids for 30–45 min. Degradation of cellulose by acids to reach LODP is known to occur through the degradation of the gylcosidic bonds of cellulose chains. Table 2 shows the LODP of the MCC prepared from the different pulps using HCl or H_2SO_4. The results are compared to a commercial MCC.

The LODP obtained for MCC BH was higher than that of MCC RH and was comparable to that of the commercial MCC. The LODP values were higher for MCC samples prepared from HCl hydrolysis than in case of using H_2SO_4 hydrolysis. Theoretically, no difference in DP is expected for using both acids, but hydrolysis via H_2SO_4 is known to cause esterification of cellulose and introduction of sulfate groups. The sulfate groups on MCC will be ionized in solution

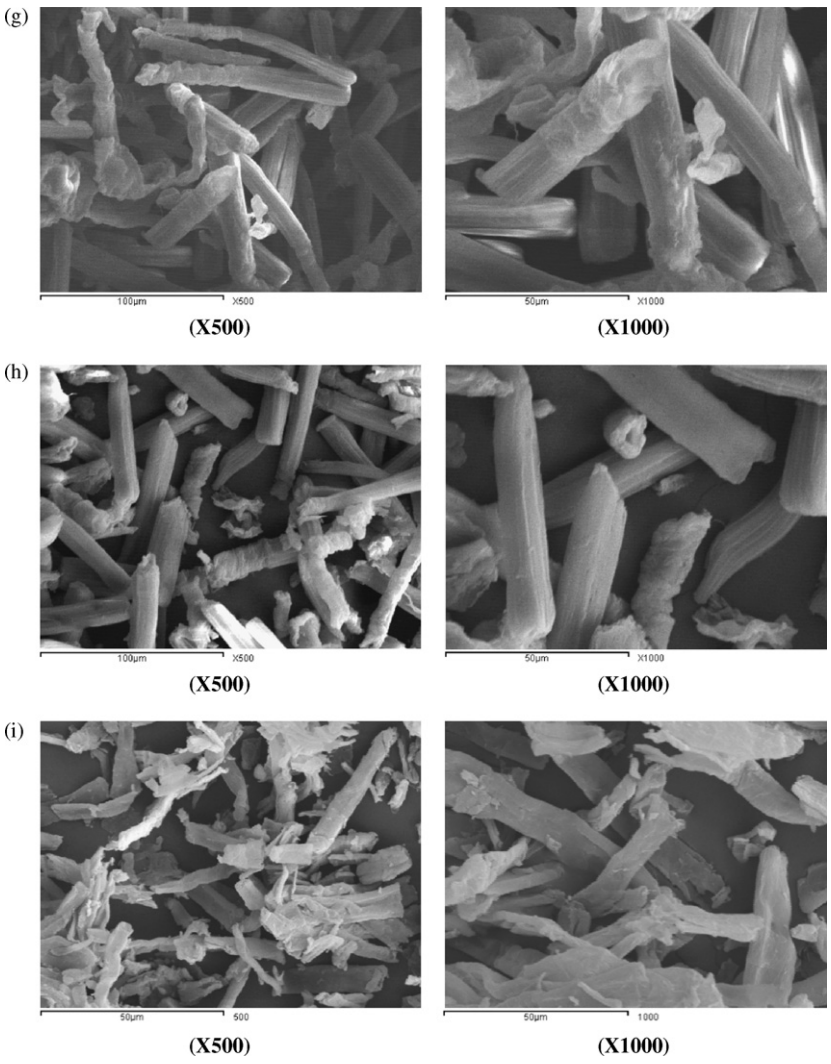

Fig. 3. (*Continued*).

and repulsion between chains may cause easier flow than MCC prepared using hydrolysis via HCl, i.e. shorter flow time and lowering in calculated DP in case of MCC prepared using H_2SO_4 (El-Sakhawy & Hassan, 2007).

3.2. Crystallinity and crystallite size

The X-ray diffraction pattern of bleached and MCC samples prepared from RH and BH compared with that of the commercial MCC sample is shown in Fig. 1(a) and (b). The calculated crystallinity index and crystallite size of the different MCC samples are given in Table 2. Both treatments, and in particular acid hydrolysis, caused a significant increase in cellulose fraction CrI values for all the lignocellulosic materials studied.

Table 2
LODP, crystallinity index (CrI) and crystallite size (L) of bleached pulp and MCC samples.

Sample	D.P.	CrI	*L* (nm)
B RH_I	565	80	5.77
MCC RH_I	163	87	5.77
B RH_{II}	407	80	5.77
MCC RH_{II}	151	82	7.05
B BH_I	568	89	7.94
MCC BH_I	285	90	9.07
B BH_{II}	336	87	9.07
MCC BH_{II}	190	92	9.07
Commercial MCC	225	85	7.94

$BRH_{I,II}$ means (bleached rice hulls pretreated with HCl and H_2SO_4 acids, respectively); $BBH_{I,II}$ means (bleached bean hulls pretreated with HCl and H_2SO_4 acids, respectively); MCC $RH_{I,II}$ means (microcrystalline cellulose prepared from rice hulls hydrolyzed via HCl and H_2SO_4 acids, respectively) and MCC $BH_{I,II}$ means (microcrystalline cellulose prepared from bean.

As shown in Fig. 1(a) and (b) all samples have a typical crystal lattice for cellulose I, which arises from the fact that there is no doublet in the intensity of the mean peak (Morán, Alvarez, Cyras, & Vázquez, 2008). Also, BBH, BRH and their MCC samples had different CrI values. For BRH and its MCC samples had CrI lower than BBH and its MCC samples regardless the kind of acid used. The degree of crystallinity of the MCC products varied from 82% to 92%. By means of Scherrer's equation, applied to the principal (100% intensity) 0 0 2 peak, the average particle size of the bleached rice hull (BRH) is the same as crystallite size of MCC RH_I while B BH_I had the same crystallite size as commercial MCC. However, MCC RH_I had the smallest crystallite size followed by MCC RH_{II} which are both smaller than the relative one obtained on a commercial MCC, while both MCC BH had the largest crystallite size.

3.3. Particle size analysis

The result of particle size analysis is shown in Table 3. The particle size is in the range of 50–500 μm. It is observed that more than 80% of the 20 g sample passed through sieve aperture 125 μm. This shows that more of the particles have sizes less than 125 μm while

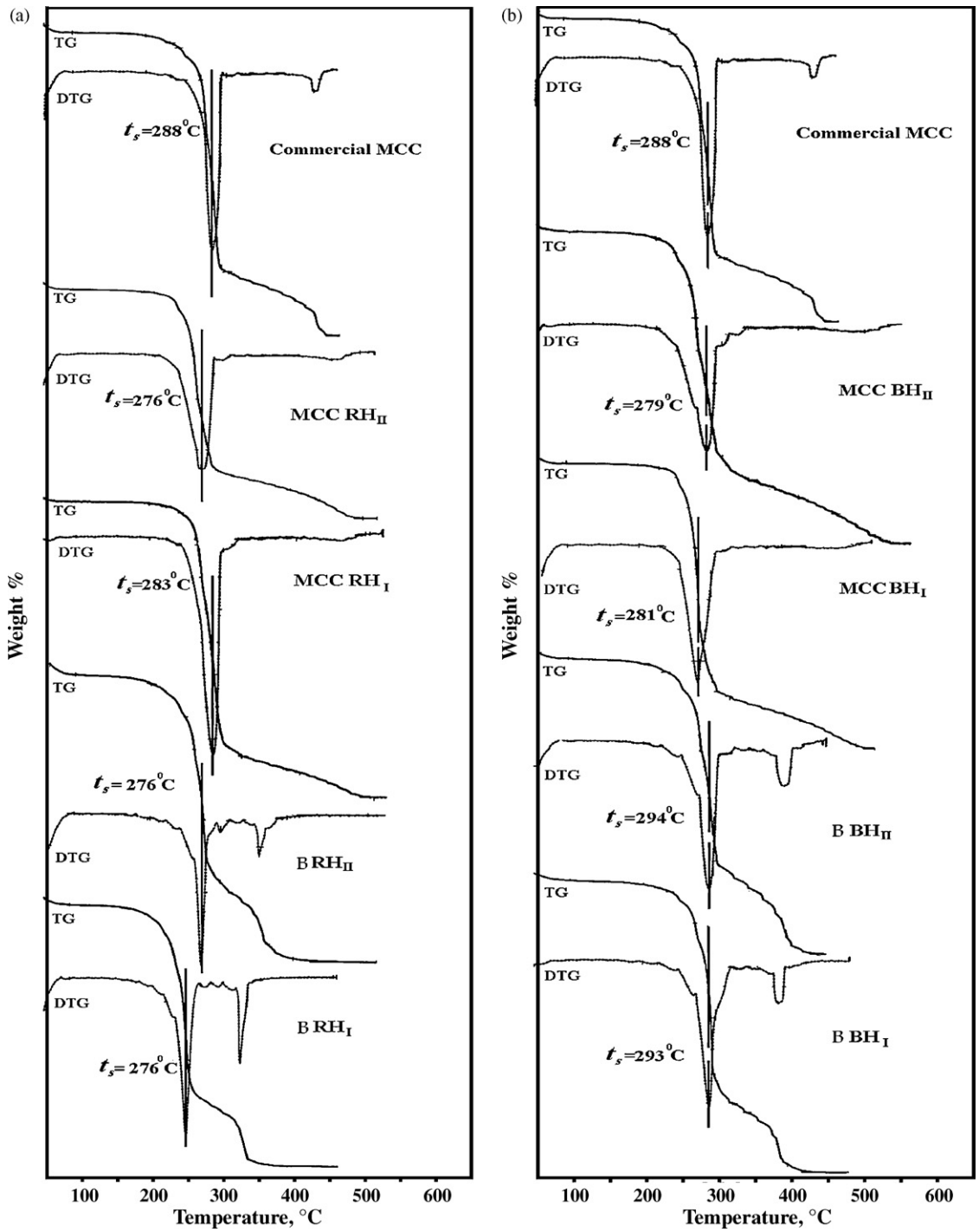

Fig. 4. (a) and (b) TG and DTG profile of: BRH_I, BRH_{II}, $MCCRH_I$, $MCCRH_{II}$, BBH_I, BBH_{II}, MCC BH_I, MCC BH_{II} and Commercial MCC.

the coarset portion has the least quantity. The calculated average diameter was 115, 114, 71, 93, and 86 μm for commercial MCC, MCC $RH_{I,II}$ and MCC $BH_{I,II}$, respectively. As shown from the table the average diameter of prepared MCC samples via HCl hydrolysis are comparable to commercial MCC, consequently, the kind of acid used affect on the average diameter of the prepared MCC samples.

3.4. FTIR spectra

The FTIR spectra were carried out to characterize the chemical structure by identifying the functional groups present in each sample. The relative absorbance of different bands was determined via the baseline correction method for making a comparative study of the spectra (Sun, Tomkinson, Wang, & Xiao, 2000; Adel, 2007). The band at 1164 cm^{-1} can be attributed to the C–O–C asymmetric valence vibration. This band has been chosen as an internal standard to determine the relative absorbance.

The IR spectra of Commercial MCC, BRH, BBH, MCC RH and MCC BH prepared using acid hydrolysis (hydrochloric and sulfuric acid 2N) are shown in Fig. 2 and Table 4.

The spectra for the bleached (RH and BH) and MCC prepared from (RH and BH) are similar to that of commercial MCC with respect to characteristic cellulose peaks and the absence of characteristic lignin peaks.

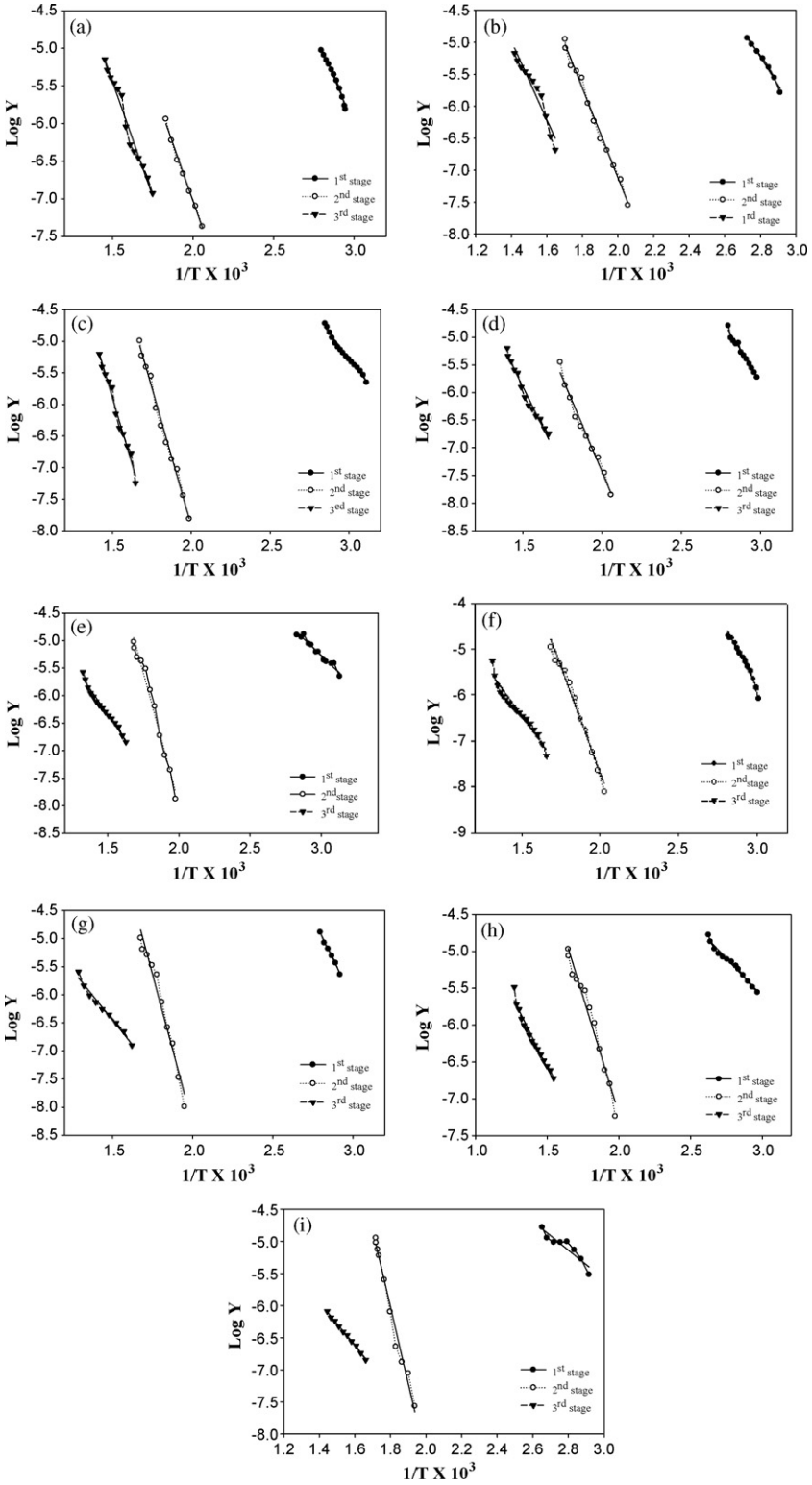

Fig. 5. Coats–redfern plots of (a) BRH_I; (b) BRH_{II}; (c) BBH_I; (d) BBH_{II}; (e) MCC RH_I; (f) MCC RH_{II}; (g) MCC BH_I; (h) MCC BH_{II} and (i) commercial MCC.

The band at 3460–3412 cm^{-1} is attributed to the hydrogen bonded O–H stretching vibration; its relative absorbance intensity decreased upon hydrolysis of ($BRH_{I,II}$) and ($BBH_{I,II}$). This is due to the degradation of the hydrogen bond between the cellulosic chains during the hydrolysis process.

The C–H stretching vibration absorbance intensity ratio at 2900 cm^{-1} is decreased upon acid hydrolysis of bleached rice and bean hulls; this is due to the presence of $–CH_2$ moieties in the MCC samples.

The absorption band at 1640 cm^{-1} attributed to the vibration of adsorbed water molecules and also to the carbonyl groups has a lower absorbance intensity ratio; this peak could be due to the presence of small amounts from hemicellulose. The presence of this peak may be arising from the opened terminal glycopyranose

Table 3
Weight fraction distribution and average diameter of the different prepared MCC samples.

Sample	Weight % retained at the mean sieve aperture					Average diameter (μm)
	500 μm	400 μm	250 μm	125 μm	50 μm	
Com. MCC	0	11.2	5.57	19.3	63.93	115
MCC RH_I	5.81	3.25	7.58	15.63	67.74	114
MCC RH_{II}	1.35	0.76	2.76	9.45	85.68	71
MCC BH_I	4.76	2.3	4.03	7.45	81.68	93
MCC BH_{II}	1.84	2.87	5.83	7.98	81.48	86

rings or oxidation of the C–OH groups. Lojewska et al. observed OH bending of adsorbed water at 1640 cm^{-1} (Lojewska, Miskowiec, Lojewski, & Pronewicz, 2005). FTIR spectra were developed after the same carefully drying process, however the water adsorbed in the cellulose molecules is very difficult to extract due to the cellulose–water interaction.

All the relative intensities of bands related to –CH or $–CH_2$ vibrations (1430, 1370, 1315 cm^{-1}) decreased, indicating an increase of the oxidation degree. The relative intensities of bands related to the ring stretching (1115, 1058 cm^{-1}) are enhanced by the hydrolysis indicating that the pyranose ring is almost unaltered in MCC samples (Bouchard, Abatzoglou, Chornet, & Overend, 1989).

The band at about 900 cm^{-1} is attributed to the asymmetric out of plane ring stretching in cellulose due to the β-linkage and also to the amorphous form in the cellulose; its absorbance intensity ratio increased due to the hydrolysis of bleached rice and bean hulls; this is probably due to elimination reaction giving alkenes. The experimental data show clearly that a portion of the solid cellulose is chemically and structurally modified in the polymeric state by acid hydrolysis and cannot be considered to be the same as the original cellulose. The modified cellulose (MCC) appears to be the product of an oxidative mechanism of hydroxyl groups implying carbonyl group formation without altering the pyranose ring structure.

Table 5
Crystallinity index (CrI), lateral order index (LOI), and moisture index (MI) of bleached pulps and MCC samples.

Sample	CrI A1370/A2900	LOI A1430/A900	MI A1640/A2903
BRH_I	0.893	2.176	0.751
MCC RH_I	1.058	1.235	0.730
BRH_{II}	0.979	2.82	0.875
MCC RH_{II}	1.034	2.146	0.522
BBH_I	0.947	2.048	0.566
MCC BH_I	1.063	1.887	0.476
BBH_{II}	0.8977	2.234	0.525
MCC BH_{II}	1.07	1.911	0.446
Commercial MCC	1.083	2.332	0.397

Table 5 shows the crystallinity index (CrI), lateral order index (LOI), and moisture index (MI) of bleached pulps and its MCC samples compared with commercial MCC. It was found that, the absorbance ratio of the bands at 1370 and 2900 cm^{-1} proposed by Nelson et al. was used to determine the crystallinity index (CrI) of cellulose material (Nelson & O'Connor, 2003). The lateral order index (LOI) was evaluated using the ratio of the absorbance at 1430 and 898 cm^{-1} (Oh, Yoo, Shin, & Kim, 2005). As shown in Table 5, bleached pulps ($BRH_{I,II}$, and $BBH_{I,II}$) have similar crystallinity but MCC samples prepared from bean hulls have crystallinity index greater than that of rice hulls and coincidental for commercial MCC. The sequence of the values of (LOI) and (MI) is different from the (CrI) for the samples. The (LOI) and (MI) for prepared MCC sampled were lower than that of its bleached samples. This may be related

Table 4
Infrared spectra, relative intensity, and assignments of different bands for bleached RH and BH materials and their MCC samples.

Band position (cm^{-1})	Relative intensity									Band assignments
	BRH_I	MCC RH_I	BRH_{II}	MCC RH_{II}	BBH_I	MCC BH_I	BBH_{II}	MCC BH_{II}	MCC Commercial	
3400	1.31	1.12	1.42	1.22	1.16	1.196	1.22	1.91	1.26	O–H stretching vibration (hydrogen bonded)
2900	0.93	0.71	0.80	0.61	0.74	0.814	0.90	0.81	0.57	CH_2, CH_2OH in cellulose in C_6
1640	0.68	0.53	0.69	0.32	0.42	0.39	0.47	0.36	0.23	Adsorbed water, C=O stretch
1430	0.82	0.69	0.80	0.56	0.69	0.70	0.75	0.70	0.53	CH_2 of pyran ring symmertric scissoring; OH plane deformation vibration {C–H deformations; asymmetric in $–CH_3$ and $–CH_2–$}
1370	0.83	0.75	0.78	0.64	0.75	0.77	0.81	0.77	0.61	CH deformation vibration or CH_2 vibration
1315	0.64	0.73	0.67	0.60	0.70	0.73	0.76	0.72	0.59	CH_2 rocking vibration
1115	1.07	1.11	1.01	1.15	1.16	1.14	1.13	1.14	≈1.20	A symmetric in-phase ring stretching, C–C and C–O stretching
1058	0.22	1.25	1.32	1.36	1.23	1.25	1.20	1.25	1.43	Pyranose ring skeletal; C_{alkyl}–O ether vibrations, and β-O-4
≈900	0.07	0.565	0.26	0.29	0.36	0.35	0.33	0.37	0.23	C–H out of plane ring stretching in cellulose due to β-linkage

(BRH_I, BBH_I) and (BRH_{II} and BBH_{II}): means bleached rice and bean hulls pretreated with HCl and H_2SO_4, respectively. (MCC RH_I, MCC BH_I) and (MCC RH_{II} and MCC BH_{II}): Microcrystalline cellulose prepared from rice and bean hulls hydrolyzed via HCl and H_2SO_4 respectively.

Table 6
Mechanical properties of tablets made from MCC samples.

Sample	Tensile strength (MPa)	Hardness (MPa)	Density (g/cm^3)
Commercial MCC	1.99	54.43	1.515
MCC RH_I	1.91	39.33	1.500
MCC RH_{II}	2.03	47.17	1.520
MCC BH_I	1.16	35.70	1.480
MCC BH_{II}	1.19	39.72	1.515

to the degradation of the hydrogen bonds between the cellulosic chains during the hydrolysis process and also an oxidation of C–OH groups take place by the hydrolysis.

3.5. Scanning electron microscopy (SEM)

SEM graphs show the morphology of the bleached pulps and different MCC samples. As seen from Fig. 3(a)–(i), after the hydrolysis of bleached pulps using 2N hydrochloric and sulfuric acids, the MCC obtained showing short fibers strands which appeared like rod-shaped MCC samples. The MCC particles appeared to be irregular fiber fragments and also show a network-structure. The shapes of the prepared MCC particles were similar to those of commercial MCC. There is no large difference between the different MCC samples except for bean hull sample which are long cylindrical and uniform in size. No significant differences were observed between samples prepared using different kind of acids was found.

3.6. Mechanical properties of MCC tablets

Source and batch variations have been reported to affect the material properties and tablet strength of MCC (Wu, Ho, & Sheu, 2001). The different MCC samples were pressed into tablets and their mechanical properties (tensile strength, and hardness) were measured. As shown in Table 6, tablets made from the prepared MCC samples had similar densities except for MCC BH_I, which produced tablets of lower density, hardness, and tensile strength.

Tablets made from MCC RH had higher tensile strength than that made from MCC BH. The difference in compatibility of rice and bean hull cellulose I powder is probably due to the difference in their DP and/or particle morphology (Reus Medina & Kumar, 2007). It has been proposed that the irregular shapes of particle which could obviously observed with SEM of RH; provide mechanical interlocking to strengthen MCC compacts (Wu et al., 2001). The hardness of MCC RH and BH tablets were comparable to each other except for MCC RH_{II} which has the nearest hardness value comparable to commercial MCC. Regarding the effect of the kind of acid used, tablets made from MCC prepared using H_2SO_4 had generally higher mechanical properties than tablets made from MCC prepared using HCl. This may be attributed to the presence of sulfate groups on MCC particles prepared using H_2SO_4. The presence of sulfate groups may increase the polar–polar interaction between the MCC particles and consequently increases the mechanical properties of tablets made from these MCC samples (El-Sakhawy & Hassan, 2007).

3.7. Thermal analysis

The following characteristic thermal parameters for each reaction step were determined from thermal analysis curves recorded for the successive steps in the decomposition process: (i) initial point temperature of the decompositions (T_i), the point at which DTG curve starts deviating from its base line. (ii) Final point temperature of decomposition (T_f), the point at which DTG curve returns to its base line. (iii) Peak temperature, i.e. temperature of maximum rate of weight loss (TDTG), the point obtained from intersection of tangents to the peak of DTG curve. (iv) The weight loss at the decomposition step (Δm) that is the amount of mass that extends from the point (T_i) up to the point (T_f) on the TG curve. The TGA curves recorded for RH and BH under all conditions are given in Fig. 4(a) and (b).

In general, the decomposition curves for RH and BH reveal a three-step decomposition process, and this observation is in accordance with those in literature (Yao, Wu, Lei, Guo, & Xu, 2008). Additionally, it is known that these three main stages were, drying (40–150 °C), removal of organic volatile matters (215–350 °C), and combustion of carbonaceous char (350–690 °C) (Markovska & Lyubchev, 2007).

The difference in thermal decomposition behavior and thermal stability for RH and BH are clearly observed after acidic (HCl and H_2SO_4) hydrolysis and can be explained by differences in chemical composition (Yaman, 2004).

3.7.1. Thermal analyses of bleached rice, bean hulls and their MCC samples

The TG curve for BRH_I and BBH_I reveal three stages of mass loss within the temperature range 61–416 °C and 43–432 °C, respectively. The first stage of degradation for BRH_I and BBH_I occurs at a temperature range 61–90 and 43–78 °C, respectively with a weight loss of 3.8% for BRH_I and 4.53% for BBH_I. The second stage was at a temperature range of 194–289 °C for BRH_I and 220–324 °C for BBH_I with a weight loss of 65.14% and 68.31%, respectively. The third stage started at about 289 °C for BRH_I and at 324 °C for BBH_I and reached a maximum at 416 °C for BRH_I and 432 °C for BBH_I with a weight loss of 23.62% and 21.84%, respectively.

Three steps for the decomposition process for BRH_{II} and BBH_{II} were observed and characterized. The first stage of degradation started at 64 °C with a weight loss of 5.96% for BRH_{II} and at 58 °C with a weight loss of 3.61% for BBH_{II}. The second stage took place in the temperature range 203–314 °C for both BRH_{II} and 203–308 °C BBH_{II} with a weight loss of 64.31% and 64.01%, respectively. The third stage of decomposition occurred in the temperature range of 314–432 °C for BRH_{II} and 308–440 °C for BBH_{II} with a weight loss of 21.24% and 28.08% for BRH_{II} and BBH_{II}, respectively.

Three steps for the decomposition process for commercial MCC were observed. The first stage of degradation started at 61 °C with a weight loss of 5.82%. The second stage started at 233 °C and reached a maximum at 309 °C with a weight loss of 71.06%. The third stage of decomposition occurred in the temperature range 309–448 °C with a weight loss of 20.06%.

Three steps for the decomposition process for MCC RH_I and MCC BH_I after hydrolysis with HCl were observed. The first stage of degradation started at 43 °C with a weight loss of 2.91% for MCC RH_I and at 63 °C with a weight loss of 3.30% for MCC BH_I. The second stage started at 223 °C for MCC RH_I and 230 °C for MCC BH_I and reached a maximum at 321 °C for MCC RH_I and 324 °C for MCC BH_I with a weight loss of 77.38% and 74.74%, respectively. The third stage of decomposition occurred in the temperature range 321–488 °C for MCC RH_I and 324–514 °C for MCC BH_I with a weight loss of 13.21% and 17.53%, respectively.

Similarly to the HCl hydrolysis, the decomposition process for MCC RH_{II} and MCC BH_{II} after hydrolysis with H_2SO_4 occurred in three stages; the first stage of degradation started at 57 °C with a weight loss of 4.65% for MCC RH_{II} and at 56 °C with a weight loss of 4.15% for MCC BH_{II}. The second stage started at 216 °C for MCC RH_{II} and 213 °C for MCC BH_{II} and reached a maximum at 320 °C and 334 °C with a weight loss of 72.23% and 74.01%, respectively. The third stage started at 320 °C for MCC RH_{II} and 334 °C for MCC BH_{II} and reached a maximum at 488 °C for MCC RH_{II} and 517 °C for MCC BH_{II} with a weight loss of 17.58% and 19.52%, respectively.

Tables 7 and 8 present the characteristic thermal and kinetic parameters data obtained from the TA curves for each step in the decomposition sequence of the materials under study.

Table 7
Thermoanalytical and thermodynamic data of the thermal decomposition steps of bleached rice and bean hulls.

Sample	Stage	TG range (°C)	DTGA peak (°C)	Estim.mass loss (%)	A (s^{-1})	ΔS^* ($JK^{-1}\,mol^{-1}$)	ΔH^* ($kJ\,mol^{-1}$)	ΔG^* ($kJ\,mol^{-1}$)	E^* ($kJ\,mol^{-1}$)
BRH_I	I	61–90	64	3.80	8.58×10^{13}	0.0208	82.89248	75.87944	85.69445
	II	194–289	276	65.14	5.84×10^{11}	−0.0247	112.2189	125.8013	116.7835
	III	289–416	358	23.62	2.19×10^{10}	−0.0532	112.011	145.5729	117.2574
									$\Sigma E = 319.7354$
BRH_{II}	I	64–97	64	5.96	4.82×10^{11}	−0.0223	69.03299	76.54231	71.83496
	II	203–314	276	64.31	1.59×10^{13}	0.0028	126.1211	124.6108	130.6857
	III	314–432	353	21.24	1.17×10^{06}	−0.1350	61.6981	146.1787	66.90295
									$\Sigma E = 269.4236$
BBH_I	I	43–78	65	4.53	2.03×10^{10}	−0.0487	62.58589	79.0331	65.39618
	II	220–324	293	68.31	9.21×10^{15}	0.0554	159.0859	127.734	163.7918
	III	324–432	385	21.84	7.16×10^{12}	−0.0054	147.9928	151.5506	153.4637
									$\Sigma E = 382.6517$
BBH_{II}	I	58–85	61	3.61	1.50×10^{11}	−0.0319	64.1129	74.76601	66.88993
	II	203–308	294	64.01	6.15×10^{12}	−0.0054	125.2656	128.3443	129.9799
	III	308–440	397	28.08	5.83×10^{09}	−0.0647	110.1859	153.5351	115.7566
									$\Sigma E = 312.6264$

$BRH_{I,II}$ means (bleached rice hulls pretreated with HCl and H_2SO_4 acids, respectively) and $BBH_{I,II}$ means (bleached bean hulls pretreated with HCl and H_2SO_4 acids, respectively).

3.7.2. Kinetics of thermal decomposition

The pyrolysis process for the materials under study may be represented by the following reaction scheme:

$$\text{Materials} \rightarrow \text{Solid residue} + \text{Volatiles}$$

Kinetic studies based on the weight-loss data were obtained by TG curve analysis. The activation energy (ΔE^*), of the various decomposition stages for the materials were determined using the Coats–Redfern equation in the following form:

$$\log\left[\frac{\log\{W_f/(W_f-W)\}}{T^2}\right] = \log\left[\frac{AR}{\theta E^*}\left(1-\frac{2RT}{E^*}\right)\right] - \frac{E^*}{2.303RT}$$

where W_f and W are the final and actual weight of the sample, respectively up to temperature T, R is the gas constant, E^* is the activation energy, θ is the heating rate and $(1-(2RT/E^*)) \cong 1$. Plotting of the left-hand side of this equation against $1/T$ gives a slope, from the intercept and linear slope of each stage, the (A; the pre-exponential factor) and (E^*) values were determined. The other kinetic parameters; the enthalpy of activation (ΔH^*), the entropy of activation (ΔS^*), and the free energy change of activation (ΔG^*) were calculated using the relationships:

$$\Delta H^* = E^* - RT;\ \Delta G^* = \Delta H^* - T\Delta S^* \text{ and } \Delta S^* = 2.303\left(\log\frac{Ah}{KT}\right)R$$

where (k) and (h) are Boltzman and Planck constants, respectively.

As can be seen from Fig. 5(a)–(i) and Tables 7 and 8, the decomposition curves of the bleached materials, commercial MCC and MCC samples after acidic hydrolysis start at a temperature of 43–64 °C. The first step of the decomposition process started in the same temperature range (43–64 °C for RH samples (bleached and MCC) and 43–63 °C for BH samples (bleached and MCC). This step was completed at 97, 108 and 104 °C for RH, BH samples and commercial MCC sample, respectively. The slight estimated mass loss at this temperature range, 2.91–5.96% for RH samples, 3.3–4.53% for BH samples and 5.82% for commercial MCC samples, may be due to evolution of absorbed water in the sample and external water bonded by surface tension (Genieva, Turmanova, Dimitrova, & Vlaev, 2008). This step was followed by a second decomposition process in which the major weight loss was 64.31–77.38% for RH samples, 64.01–74.74% for BH samples and 71.06% for commercial MCC sample. This weight loss was estimated within a temperature range 194–314 °C, 203–334 °C and

Table 8
Thermoanalytical and Thermodynamic data of the thermal decomposition steps of MCC samples.

Sample	Stage	TG range (°C)	DTGA peak (°C)	Estim.mass loss (%)	A(s^{-1})	ΔS^* ($JK^{-1}\,mol^{-1}$)	ΔH^* ($kJ\,mol^{-1}$)	ΔG^* ($kJ\,mol^{-1}$)	E^* ($kJ\,mol^{-1}$)
MCC RH_I	I	43–86	64	2.91	$1.09X10^{08}$	−0.0921	42.79857	73.84159	45.60055
	II	223–321	283	77.38	4.33×10^{20}	0.1450	206.6664	126.0461	211.2892
	III	321–488	464	13.21	2.89×10^{06}	−0.1288	75.26159	170.1766	81.38936
									$\Sigma E = 338.2791$
MCC RH_{II}	I	57–82	62	4.65	7.56×10^{17}	0.0964	105.72	73.42583	108.5054
	II	216–320	276	72.23	$1.80\times\times10^{11}$	−0.0345	105.4347	124.3819	109.9993
	III	320–488	460	17.58	1.48×10^{04}	−0.1726	49.16498	175.686	55.25949
									$\Sigma E = 273.7641$
MCC BH_I	I	63–94	64	3.30	2.55×10^{12}	−0.0084	72.74334	75.58692	75.54532
	II	230–324	281	74.74	7.27×10^{19}	0.1302	199.6479	127.5242	204.2542
	III	324–514	477	17.53	7.01×10^{05}	−0.1407	68.91807	174.445	75.15393
									$\Sigma E = 354.9534$
MCC BH_{II}	I	56–108	58	4.15	3.71×10^{07}	−0.1009	42.39828	75.79818	45.15038
	II	213–334	279	74.01	8.52×10^{12}	−0.0025	125.6186	126.9947	130.2081
	III	334–517	487	19.52	6.96×10^{06}	−0.1217	83.0163	175.5244	89.3353
									$\Sigma E = 264.6938$
MCC	I	61–104	63	5.82	4.40×10^{09}	−0.0613	55.5778	76.1741	58.37146
	II	233–309	288	71.06	2.34×10^{22}	0.1781	224.0573	124.1484	228.7218
	III	309–448	428	20.06	1.40×10^{05}	−0.1535	59.0988	166.71	64.92724
									$\Sigma E = 352.0205$

MCC $RH_{I,II}$ means (microcrystalline cellulose prepared from rice hulls hydrolyzed via HCl and H_2SO_4 acids, respectively); MCC $BH_{I,II}$ means (microcrystalline cellulose prepared from bean hulls hydrolyzed via HCl and H_2SO_4 acids, respectively) and MCC means commercial microcrystalline cellulose.

233–309 °C for RH, BH and commercial MCC samples, respectively.

This temperature range is referred to as the active pyrolysis zone which can be attributed to the decomposition behaviors of the major constituents of the materials under study: cellulose, hemicellulose, lignin and ash. Since hemicelluloses and cellulose components are degraded first, they are the main contributors to the evolution of the volatile compounds, while lignin is degraded later and mainly responsible for the char portion of the product and the thermal degradation properties (Genieva et al., 2008; Yao et al., 2008). Accordingly, the major weight loss obtained at the above temperature range is attributed to the decomposition of primary hemicelluloses and cellulose. The thermal decomposition process was completed by a third step occuring at a temperature range of 289–488 °C, 308–517 °C and 309–448 °C for RH, BH and commercial MCC samples, respectively. This temperature range is referred to as the passive pyrolysis zone and the smaller estimated mass loss of 13.21–23.62%, 17.53–28.08% and 20.06% for RH, BH and commercial MCC samples, respectively at this temperature range compared to the obtained in the second stage is attributed to lignin conversion.

4. Conclusion

Residues from annual plants such as rice and bean hulls are interesting alternatives as cellulose source for several applications. Sch materials are renewable and vastly available in many regions of the world, and are generally burned or disposed for ambient degradation. Rice and bean hulls could be used for the preparation of MCC using either HCl or H_2SO_4 hydrolysis. The kind of acid used was found to affect degree of polymerization, crystallinity, tensile strength, thermal stability, hardness of the tablets and morphology of the fibers. MCC prepared in this work from cellulose extracted from RH and BH has properties similar to that of commercial MCC.

References

Adel, A. M. (2007). Characterization and aging of bio-treated kraft bagasse pulp. *Journal of Applied Polymer Science*, *104*, 1887–1894.

Adel, A. M., Abd El-Wahab, Z. H., Ibrahim, A. A., & Al-Shemy, M. T. (2010). Characterization of microcrystalline cellulose prepared from lignocellulosic materials. Part I. Acid catalyzed hydrolysis. *Bioresource Technology*, *101*, 4446–4455.

Bouchard, J., Abatzoglou, N., Chornet, E., & Overend, R. P. (1989). Characterization of depolymerized cellulosic residues. Part I: Residues obtained by acid hydrolysis process. *Wood Science and Technology*, *23*, 343–355.

Browning, B. L. (1967). *Methods of wood chemistry* (pp. 387–882). New York: Interscience.

Ejikeme, P. M. (2008). Investigation of the physicochemical properties of microcrystalline cellulose from agricultural wastes I: Orange mesocarp. *Cellulose*, *15*, 141–147.

El-Sakhawy, M., & Hassan, M. L. (2007). Physical and mechanical properties of microcrystalline cellulose prepared from agricultural residues. *Carbohydrate Polymers*, *67*, 1–10.

Genieva, S. D., Turmanova, S. Ch., Dimitrova, A. S., & Vlaev, L. T. (2008). Characterization of rice husks and the products of its thermal degradation in air or nitrogen atmosphere. *Journal of Thermal Analysis and Calorimetry*, *93*(2), 387–396.

Gümüskaya, E., Usta, M., & Kirci, H. (2003). The effects of various pulping conditions on crystalline structure of cellulose in cotton linters. *Polymer Degradation and Stability*, *81*, 559–564.

Hanna, M., Blby, G., & Miladinove, V. (2001). Production of microcrystalline cellulose by reactive extrusion, US Patent 6,228,213.

He, J., Tang, Y., & Wang, S.-Y. (2007). Differences in morphological characteristics of bamboo fibres and other natural cellulose fibres: Studies on X-ray diffraction, solid state 13C-CP/MAS NMR, and second derivative FTIR spectroscopy data. *Iranian Polymer Journal*, *16*(12), 807–818.

Jain, J. K., Dixit, V. K., & Varma, K. C. (1993). Preparation of microcrystalline cellulose from cereal straw and its evaluation as a tablet excipient. *Indian Journal of Pharmaceutical Science*, *45*, 83–85.

Laka, M., & Chernyavskaya, S. (2007). Obtaining microcrystalline cellulose from softwood and hardwood pulp. *Bioresources*, *2*(3), 583–589.

Lojewska, J., Miskowiec, P., Lojewski, T., & Pronewicz, L. M. (2005). cellulose oxidative and hydrolysis degradation: In situ FTIR approach. *Polymer Degradation and Stability*, *88*(3), 512–520.

Markovska, I. G., & Lyubchev, L. A. (2007). A study on the thermal destruction of rice husk in air and nitrogen atmosphere. *Journal of Thermal Analysis and Calorimetry*, *89*(3), 809–814.

Morán, J. I., Alvarez, V. A., Cyras, V. P., & Vázquez, A. (2008). Extraction of cellulose and preparation of nanocellulose from sisal fibers. *Cellulose*, *15*, 149–159.

Nelson, M. L., & O'Connor, R. T. (2003). Relation of certain infrared bands to cellulose crystallinity and crystal lattice type. Part II. A new infrared ratio for estimation of crystallinity in celluloses I and II. *Journal of Applied Polymer Science*, *8*, 1325–1341.

Ofoefule, S. I., & Chukwu, A. (1999). Application of blends of MCC – Cissus gum in the formation of aqueous suspensions. *Bollettino Chimico Farmaceutico*, *138*(5), 217–222.

Oh, S. Y., Yoo, D. I., Shin, Y., & Kim, H. C. (2005). Crystalline structure analysis of cellulose treated with sodium hydroxide and carbon dioxide by means of X-ray diffraction and FTIR spectroscopy. *Carbohydrate Research*, *340*, 2376–2391.

Ohwoavworhua, F. O., & Adelakun, T. A. (2005). Some physical characteristics of microcrystalline cellulose obtained from raw cotton of Cochlospermum planchonii. *Tropical, Journal of Pharmaceutical Research*, *4*(2), 501–507.

Ohwoavworhua, F. O., Kunle, O. O., & Ofoefule, S. I. (2004). Extraction and characterisation of microcrystalline cellusose derived from luffa cylindrica plant. *African Journal of Pharmaceutical Research and Development*, *1*(1), 1–6.

Okhamafe, A. O., Ejike, E. N., Akinrinola, F. F., & Ubane-Ine, D. (1995). Aspect of tablet disintegrant properties of cellulose derived from Bagasse and Maize Cob. West African. *Journal of Pharmacy*, *9*(1), 8–13.

Okhamafe, A. O., Igboechi, A., & Obaseki, T. O. (1991). Celluloses extracted from groundnut shell and rice husks 1. Preliminary physicochemical characterization. *Pharmacy World Journal*, *8*(4), 120–130.

Paralikar, K. M., & Bhatawdekar, S. P. (1988). Microcrystalline cellulose from bagasse pulp. *Biological Wastes*, *24*, 75–77.

Picker-Freyer, K. M. (2007). An insight into the process of tablet formation of microcrystalline structural changes on a nanoscale level. *Journal of Thermal Analysis and Calorimetry*, *89*(3), 745–748.

Reus Medina, M., & Kumar, V. (2007). Comparative evaluation of powder and tableting properties of low and high degree of polymerization cellulose I and cellulose II excipients. *International Journal of Pharmaceutics*, *337*, 202–209.

Sun, C. C. (2008). Mechanism of moisture induced variations in true density and compaction properties of microcrystalline cellulose. *International Journal of Pharmaceutics*, *346*, 93–101.

Sun, R. C., Tomkinson, J., Wang, Y., & Xiao, w. B. (2000). Physico-chemical and structural characterization of hemicelluloses from wheat straw by alkaline peroxide extraction. *Polymer*, *41*, 2647–2656.

Uesu, N. Y., Pineda, E. A. G., & Hechenleitner, A. A. W. (2000). Microcrystalline cellulose from soybean husk: Effects of solvent treatments on its properties as acetylsalicylic acid carrier. *International Journal of Pharmaceutics*, *206*, 85–96.

Wise, L. E., Murphy, M., & D'Addieco, A. A. (1946). Chlorite hollocellulose its fractionation and beating on summative wood analysis and on studies on the hemicelluloses. *Paper Trade Journal*, *122*(2), 35.

Wu, J.-S., Ho, H.-O., & Sheu, M.-T. (2001). A statistical design to evaluate the influence of manufacturing factors and material properties on the mechanical performances of microcrystalline cellulose. *Powder Technology*, *118*, 219–228.

Yaman, S. (2004). Pyrolysis of biomass to produce fuels and chemical feedstocks. *Energy Conversion and Management*, *45*, 651–671.

Yao, F., Wu, Q., Lei, Y., Guo, W., & Xu, Y. (2008). Thermal decomposition kinetics of natural fibers: Activation energy with dynamic thermogravimetric analysis. *Polymer Degradation and Stability*, *93*, 90–98.